BMB
reports

Multiple hTAF$_{II}$31-binding motifs in the intrinsically unfolded transcriptional activation domain of VP16

Do-Hyoung Kim[1,#], Si-Hyung Lee[1,#], Ki Hoon Nam[1,3], Seung-Wook Chi[2], Iksoo Chang[3] & Kyou-Hoon Han[1,]*

[1]Bioinformatics Research Center, [2]Medical Proteomics Research Center, KRIBB, Daejeon 305-806, [3]Computational Proteomics and Biophysics Laboratory, Department of Physics, Pusan National University, Busan 609-735, Korea

Transcriptional activation domain (TAD) in virion protein 16 (VP16) of herpes simplex virus does not have any globular structure, yet exhibits a potent transcriptional activity. In order to probe the structural basis for the transcriptional activity of VP16 TAD, we have used NMR spectroscopy to investigate its detailed structural features. Results show that an unbound VP16 TAD is not merely "unstructured" but contains four short motifs (residues 424-433, 442-446, 465-467 and 472-479) with transient structural order. Pre-structured motifs in other intrinsically unfolded proteins (IUPs) were shown to be critically involved in target protein binding. The 472-479 motif was previously shown to bind to hTAF$_{II}$31, whereas the hTAF$_{II}$31-binding ability of other motifs found in this study has not been addressed. The VP16 TAD represents another IUP whose pre-structured motifs mediate promiscuous binding to various target proteins. [BMB reports 2009; 42(7): 411-417]

INTRODUCTION

Transcriptional activation domains (TADs) are important functional modules within transcriptional activators: initiation of transcription depends on the ability of TADs to recruit various components of transcription machinery (1-3). Several types of TADs have been described based upon their amino acid composition (1). Even though structural features have been described for a few "acidic" TADs that are rich with Asp and Glu, the structural basis for TAD-target protein interaction is yet to be fully understood. p53 TAD is a well-known acidic TAD that does not form a unique tertiary structure, existing in a mostly unstructured (MU) state (4). Other acidic TADs were also found to be in a similar structural state (5-7). In fact, TADs constitute an important sub-family of what is known as intrinsically unfolded/disordered proteins (IUPs/IDPs).

*Corresponding author. Tel: 82-42-860-4250; Fax: 82-42-860-4259; E-mail: khhan600@kribb.re.kr
#These authors contributed equally to this work.

Received 9 December 2008, Accepted 13 February 2009

Keywords: Herpes simplex virus, hTAF$_{II}$31, Intrinsically unfolded protein, NMR, Transcriptional activation domain, VP16

The TAD in the virion protein 16 (VP16) of herpes simplex virus is located at the C-terminus of VP16 (residues 412-490) and is an acidic TAD having 17 Asp and 5 Glu (8). It is responsible for activation of viral immediate early genes and strongly transactivates relevant genes when fused to the DNA-binding domains of other transactivators (9). This 79-residue TAD can be further divided into two sub-domains, an N-terminal sub-domain (residues 412-453) and a C-terminal sub-domain (residues 454-490) (10). VP16 TAD contains so-called positionally-conserved hydrophobic residues such as Leu^{439}, Phe^{442}, Leu^{444}, Phe^{479} and Leu^{483} in addition to dominant acidic amino acid residues. Early studies have shown that mutation of these positionally-conserved hydrophobic residues critically influences the transcriptional activity of VP16 TAD (10, 11).

Several members in eukaryotic transcription machinery, such as TBP (12), TFIIA (13, 14), TFIIB (12), CBP (15, 16), and p300 (17, 18), bind to VP16 TAD. Human TFIID TATA box-binding protein-associated factor 31 (hTAF$_{II}$31) (19), a co-activator that interacts with various acidic transcriptional activators (20-22), also binds VP16 TAD. An early NMR study has shown that a fragment (residues 472-483) of VP16 TAD becomes an induced α-helix upon binding to hTAF$_{II}$31 (19). A recent NMR study has demonstrated that the same fragment is involved in binding to Tfb1/TFIIH (23). In addition, a human transcriptional coactivator-positive cofactor (PC4) and a general transcription factor TFIIB were reported to interact with two regions in VP16 TAD (residues 429-450 and 465-488) (24). These results suggest that the VP16 TAD utilizes more than one sub-domain for target interaction, as was shown for p53 TAD (4, 25). Thus, delineating location of pre-structured motifs in TADs and examining of their interactions with various target proteins has provided valuable insight into understanding a structural basis for TAD-target interactions or IUP-target interactions (19, 24-27). A well-known characteristic of IUPs is their binding promiscuity, which is possible mostly due to presence of transiently-structured motifs that pre-exist before target binding and are structurally primed for target recognition (25-27). Since activation domains in VP16, E2F1, and HIF-1α contain positionally-conserved hydrophobic residues, such as p53 TAD (25), it is reasonable to investigate whether these residues in VP16 TAD would also "pre-form" transiently-structured motifs, and if these motifs are important factors for

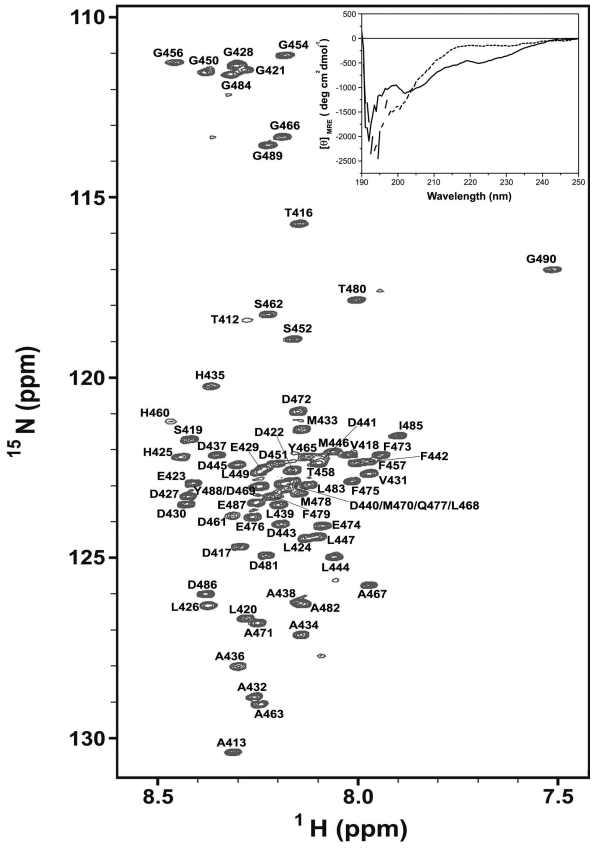

Fig. 1. An ^{15}N-^{1}H HSQC spectrum of the full-length VP16 TAD (100 μM) obtained under 50 mM sodium acetate-d_3 (pH 6.3), 50 mM NaCl, 90% H_2O/10% ^2H_2O 90% at 20°C with resonances assigned. The broken line in the insert is a CD spectrum obtained under the NMR solvent condition, whereas the solid line represents a CD spectrum obtained after adding 40% TFE to the aqueous solvent.

target binding as was demonstrated for p53 TAD (25-28). In this study, we have used multidimensional NMR methods in order to characterize detailed structural features of a full-length VP16 TAD. The N-terminal sub-domain of the VP16 TAD is found to contain hTAF$_{II}$31-binding pre-structured motifs in addition to the one identified in the C-terminal sub-domain (19).

RESULTS AND DISCUSSION

NMR analysis of VP16 TAD

Resonance assignment for the 79-residue full-length VP16 TAD was achieved using three-dimensional ^{15}N-edited NOESY-HSQC and TOCSY-HSQC spectra. All the backbone ^{15}N and ^{1}H resonances were unambiguously assigned except for four prolines. Our resonance assignment is in agreement with what was previously reported (24). Shown in Fig. 1 is a ^{15}N-^{1}H HSQC spectrum of ^{15}N-labeled VP16 TAD. The spectrum shows narrow chemical shift dispersion consistent with the findings (24, 29) that the VP16 TAD is devoid of a globular structure. An unstructured nature of the VP16 TAD is visible in its CD spectrum (the insert in Fig. 1). Shown in Fig. 2 is a summary of interproton NOEs, $^{3}J_{HNH\alpha}$ coupling constants, and H_α chemical shift index (CSI) for the full-length VP16 TAD in aqueous solution. Presence of sequential d_{NN} NOEs and helical H_α CSIs in several regions indicates that VP16 TAD is not totally unstructured, but populated with non-contiguous transient structures.

Five consecutive helical H_α CSIs and a stretch of sequential d_{NN} NOEs are observed for residues 472-476. In addition, sequential d_{NN} NOEs are observed for residues 418-425, 430-436, 442-445, 465-467 and 479-485, indicating that these residues have some propensity to form transient structures. The propensity to form transient structures increases slightly under a hydrophobic condition (Fig. 2). Shown in Fig. 3 is the backbone dynamics data for VP16 TAD where the regions showing

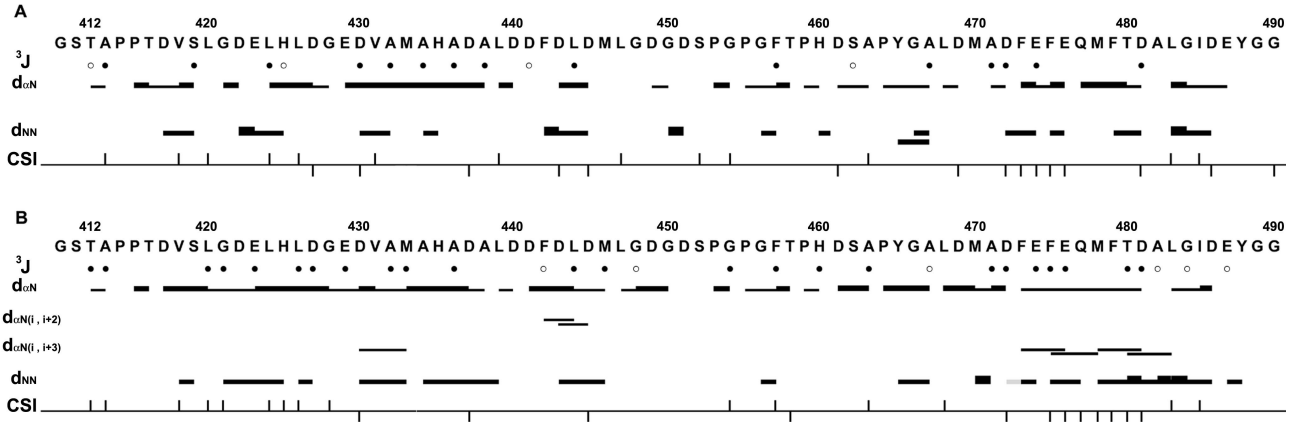

Fig. 2. Summary of interproton NOEs, $^{3}J_{HNH\alpha}$, and chemical shift index (CSI) of H_α protons for the full-length VP16 TAD in (A) H_2O and (B) 30% TFE/water (v/v) solution. The thickness of bars represents relative strength of NOEs. Filled circles are drawn when $^{3}J_{HNH\alpha} < 6$ Hz and open circles when $^{3}J_{HNH\alpha} > 8$ Hz. The filled squares above and below the horizontal line represent CSI values of +1 and -1, respectively. The gray square indicates an ambiguity due to overlapping of NOEs.

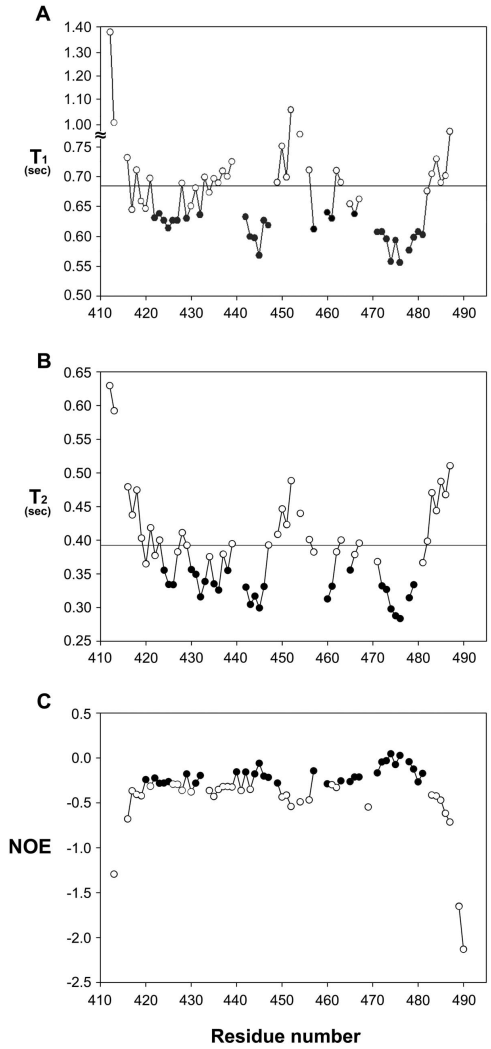

Fig. 3. Plots of backbone ^{15}N relaxation times and ^{15}N-^{1}H heteronuclear NOEs against the residue number of the full-length VP16 TAD. (A) T_1, (B) T_2 relaxation times, (C) ^{15}N-^{1}H heteronuclear NOEs. The horizontal lines in (A) and (B) indicate average values. In the regions that show local structural ordering, the heteronuclear NOE, T_1, T_2 values are displayed as black circles.

T_1/T_2 values below the average are found to overlap with the regions showing pre-structuring tendency in Fig. 2. According to backbone dynamics the propensity for structural order decreases in the following order: 472-479 > 442-446 > 424-433 ≈ 465-467. The first is a hTAF$_{II}$31-binding motif (19) as well as a Tfb1/TFIIH-binding motif (23).

The overall structural state of VP16 TAD

Given that the full-length VP16 TAD is intrinsically unstructured like p53 TAD or preS1 (4, 24, 25, 29, 30), we focused our efforts on delineating the location of pre-structured motifs within an unbound state of VP16 TAD and to examine their interactions with hTAF$_{II}$31. VP16 TAD demonstrates an IUP where its backbone dynamics serves as a useful measure for detecting pre-structuring propensity even when pre-structuring tendency based upon NOE or CSI patterns is not evident. We note that the observed pre-structured regions (residues 472-479 and 442-446) in VP16 TAD overlap with location of the positionally-conserved hydrophobic residues delineated previously (25). Another feature to note is that multiple pre-structured motifs in VP16 TAD have differing degrees of structural stability; the 472-479 region in the C-terminal sub-domain forms a relatively well-defined helix, whereas other motifs in the N-terminal sub-domain show less structural order. Such a pattern was observed in other MU type IUPs that contain more than one pre-structured motifs (4, 29). Typically, the population of transient pre-structured motifs in a mostly unstructured type of IUPs is less than 20% (4, 31). In p53 TAD where the population of transient motifs is ~10%, the CD spectral change at 220 nm caused by destruction of pre-structured motifs due to addition of denaturants could be clearly measured (28). In the case of VP16 TAD, however, where the population of transient motifs is only ~5% (the insert in Fig. 1) the CD spectral change due to denaturants is too small to be statistically meaningful; its magnitude is similar to measurement errors, rendering it difficult to detect presence and breakage of transient structural order by CD.

hTAF$_{II}$31-binding characteristics of pre-structured motifs in VP16 TAD

A few studies have elegantly demonstrated that pre-structured motifs in IUPs are involved in target protein binding (23-27, 32, 33). In order to examine whether the pre-structured motifs in VP16 TAD also mediate target protein binding, in particular, the newly delineated region (residues 423-440) in the N-terminal sub-domain of VP16 TAD, we have used surface plasma resonance technique to measure the hTAF$_{II}$31-binding affinity of the newly identified hTAF$_{II}$31-binding region (residues 423-440) as well as that of the previously identified hTAF$_{II}$31-binding region (residues 469-485). The K_d values of the former and the latter for hTAF$_{II}$31-binding are 79 μM and 11 μM, respectively (Fig. 4). A somewhat weaker affinity of the N-terminal sub-domain in VP16 TAD was also observed when VP16 TAD interacts with other target proteins (23). The p53 TAD, a well-known mostly unstructured type of IUP, also contains two sub-domains. Initially, its N-terminal sub-domain was thought to be critical for binding with target proteins, but later the pre-structured motifs in the C-terminal sub-domain turned out to be important (25-27). The fact that multiple pre-structured motifs within VP16 TAD interact with various components (hTAF$_{II}$31, PC4/TFIIB and Tfb1/TFIIH) of transcriptional machinery suggests that the transcriptional activity of VP16 TAD is strongly associated with presence of these motifs. In fact, this report constitutes another piece of evidence that presence of multiple pre-structured target-binding motifs is a general fea-

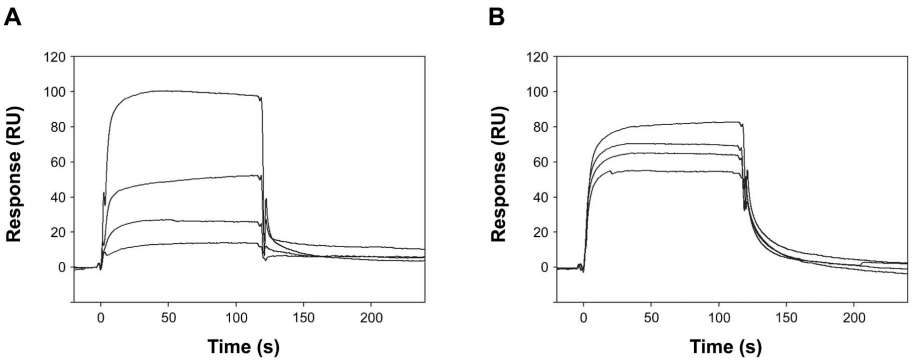

Fig. 4. Surface plasma resonance binding isotherms for the VP16 TAD peptides to hTAF$_{II}$31. Biosensograms are shown for the interaction of VP16 TAD (469-485) (A) and VP16 TAD (423-440) (B) with immobilized hTAF$_{II}$31 (1-140) as described under "Materials and methods". The concentrations of the VP16 TAD peptides are 10, 20, 40, and 80 μM in (A) and 80, 200, 240, and 320 μM in (B). RU = response units.

ture among transcriptional activation domains that contain a long intrinsically unfolded segment consisting of more than 50 amino acid residues.

Mechanism of IUP-target binding: conformational selection vs. induced-fit

While intrinsically unfolded proteins/domains (IUPs/IUDs) share a common feature of not having a uniquely defined tertiary structure, their detailed structural features appear to vary. Some are described to be "totally unstructured", lacking any trace of local structural order (34), whereas others are mostly unstructured (MU) with residual secondary structural elements (4, 23-27, 30, 35-41). For the first type, an induced fit mechanism involving a coil → helix transition seems to be needed to describe their binding to target proteins (42-49). For the second type, such as p53 TAD (4, 25-27), VP16 TAD (23, 24), ribosomal protein S4 (35), amyloid precursor protein (36), GCN4-p1 (37), p27^{Kip1} (38), c-Myb TAD (39), the σ^{28} binding domain of FlgM (40), thymosin β4 (41) and preS1 (30) slight conformational tightening of pre-structured motifs upon target binding would be sufficient.

An induced-fit mechanism was proposed to describe binding of a p53 TAD fragment (residues 15-29) to mdm2, because the putative helix formed by these residues was observed only in the x-ray structure of an mdm2-bound peptide (33). Since this helix was in fact found to be pre-formed, i.e., being significantly populated in an mdm2-free state (4) the proposed induced-fit mechanism described implicitly by a "coil → helix transition" concept is somewhat misleading. The helix observed in a hTAF$_{II}$31-bound state of VP16 TAD (residues 472-479) was also claimed to be induced (19), yet the current work has clearly demonstrated that this helix is also pre-formed or pre-structured to a significant degree. The coil → helix description was used recently (50) to consolidate the fact that the initial binding between pKID and KIX should involve induction of a helix. Ironically, such a description is not fully consistent with the NMR data reported by the same authors (51), in which one can see that the residues forming the induced helix are helically pre-structured to a significant degree in an unbound state.

The presence of pre-structured motifs in VP16 TAD and the MU type of IUPs and their involvement in target binding strongly suggests that target proteins recognize a "pre-structured" motif rather than a totally unstructured segment. Such a conformational selection mechanism for IUP-target binding process gains support from the observation that a structurally better defined motif or a more pre-structured motif exhibits a higher affinity when it competes for the same target protein against other motifs that are less pre-structured. The highly pre-structured helix motif in p53 TAD has a ~20-fold higher affinity than the structurally less primed turn II motif to the same target protein mdm2 (25, 33). A similar trend is true for the C-terminal region in VP16 TAD containing the 472-429 motif. It is more helically pre-structured and exhibits a 3-5-fold stronger affinity to hTAF$_{II}$31 or to Tfb1/TFIIH than the N-terminal sub-domain containing residues 423-440, which show a weaker pre-structuring tendency. The observed correlation between biological function and presence of pre-structured motifs in IUPs helps to establish useful structural rationale for transcriptional activity (23-27) or an ability to mediate protein-protein interactions in viral proteins (30).

MATERIALS AND METHODS

Protein preparation

A recombinant full-length VP16 TAD construct corresponding to residues 412-490 was expressed in pGEX-2T vector. The first two N-terminal residues of the recombinant protein, glycine and serine, originated from the glutathione-S-transferase fusion linker. Transformed *Escherichia coli* BL21 (DE3) cells were grown at 37°C to an OD_{600} of 0.6 and the culture was induced with 0.5 mM isopropyl thio-β-D-thiogalactopyranoside (IPTG). Then, the cells were further cultivated at 20°C for 16 h. The harvested cell suspension was sonicated in 50 mM TrisHCl (pH 8), 0.2 M NaCl, 1 mM PMSF, 10 mM β-mercaptoethanol and centrifuged for 30 min at 30,000 × g. Both ^{15}N-labeled and unlabeled VP16 TAD (412-490) were purified, using Glutathione-Sepharose column, Q-Sepharose column, and Hiprep 26/60 Sephacryl S-200 FPLC column (Amersham Pharmacia Biotech, Uppsala, Sweden). The molecular weight

of the purified VP16 TAD (412-490) was confirmed by MALDI-TOF mass spectrometry.

Peptide preparation

The VP16 TAD peptides corresponding to residues 423-440 and 469-485 were synthesized by a solid phase method with Multiple Peptide Synthesizer APEX 348 Ω (Advanced Chemtech, Louisville, KY). The C-termini of all the synthesized peptides were amidated. The peptides were purified by reverse phase HPLC using Vydac C_{18} columns and the peptide masses confirmed by MALDI-TOF mass spectrometry.

CD spectropolarimetry

CD spectra were measured with 10 μM protein samples on a JASCO J-720 spectropolarimeter using a 1 mm cell in 50 mM sodium acetate (pH 6.3), 50 mM NaCl at 20°C. Four scans were taken for each sample.

NMR spectroscopy

NMR spectra were acquired using a Varian Unity INOVA 600 and Bruker Avance II 900 spectrometers equipped with cryogenic probes. For the backbone assignment of the full-length VP16 TAD, 3D ^{15}N-edited TOCSY-HSQC and ^{15}N-edited NOESY-HSQC (τ_{mix} = 68-150 ms) were obtained at 20°C in 50 mM sodium acetate-d_3 (pH 6.3), 50 mM NaCl, 90% H_2O/10% ^2H_2O, or in 30% trifluoroethanol (TFE)/water (v/v). The H_α CSI values of -1, 0 or +1 were obtained using the method proposed by Wishart and Sykes (52). The three-bond $^3J_{HNH\alpha}$ coupling constants were measured by HNHA experiment. ^{15}N T_1 values were measured from spectra recorded with seven relaxation delays (20, 40, 80, 160, 320, 640, 1,280 ms). ^{15}N T_2 values were measured from spectra recorded using a CPMG sequence with eight relaxation delays (10, 30, 50, 70, 90, 130, 190, 250 ms) following a published method (4). The ^{15}N-^{1}H heteronuclear steady-state NOEs were measured from a pair of spectra recorded with and without a proton presaturation. All data were processed and analyzed on a Sun SPARCstation (Sun Microsystems, Inc., Santa Clara, CA) using Varian Vnmr software and nmrPipe/ nmrDraw software.

Surface plasma resonance

Surface plasma resonance experiments for the VP16 TAD (423-440) that encompasses two short motifs in the N-terminal sub-domain and the VP16 TAD (469-485) were performed in HBS buffer (10 mM HEPES (pH 7.4), 150 mM NaCl, 1 mM EDTA, and 0.005 % Tween20) with a flow rate of 20 μL/min at 25°C in a BIAcore 3000 instrument (BIAcore AB, Uppsala, Sweden). hTAF$_{II}$31 (1-140) protein in 25 mM sodium acetate (pH 4.5) was immobilized on a CM5 sensor chip using an amine coupling kit (BIAcore AB, Uppsala, Sweden). Kinetic measurements were made and kinetic constants were derived with the BIAevaluation Version 3.0 software (BIAcore AB) by fitting to a 1 : 1 Langmuir binding model.

Acknowledgements

This work has been supported by the Korea Science and Engineering Foundation (KOSEF) grant (R01-2006-000-10905-0) (K. H. & I. C.), and also by Bio-MR Research Program (use of the 900 MHz NMR facility at Korea Basic Science Institute) of MOST (E27070).

REFERENCES

1. Triezenberg, S. J. (1995) Structure and function of transcriptional activation domains. *Curr. Opin. Genet. Dev.* **5**, 190-196.
2. Tjian, R. and Maniatis, T. (1994) Transcriptional activation: a complex puzzle with few easy pieces. *Cell* **77**, 5-8.
3. Pugh, B. F. (1996) Mechanisms of transcription complex assembly. *Curr. Opin. Cell. Biol.* **8**, 303-311.
4. Lee, H., Mok, K. H., Muhandiram, R., Park, K. H., Suk, J. E., Kim, D. H., Chang, J., Sung, Y. C., Choi, K. Y. and Han, K. H. (2000) Local structural elements in the mostly unstructured transcriptional activation domain of human p53. *J. Biol. Chem.* **275**, 29426-29432.
5. Sigler, P. B. (1988) Transcriptional activation. Acid blobs and negative noodles. *Nature* **333**, 210-212.
6. Hahn, S. (1993) Structure(?) and function of acidic transcription activators. *Cell* **72**, 481-483.
7. Cho, H. S., Liu, C. W., Damberger, F. F., Pelton, J. G., Nelson, H. C. and Wemmer, D. E. (1996) Yeast heat shock transcription factor N-terminal activation domains are unstructured as probed by heteronuclear NMR spectroscopy. *Protein Sci.* **5**, 262-269.
8. Campbell, M. E., Palfreyman, J. W. and Preston, C. M. (1984) Identification of herpes simplex virus DNA sequences which encode a trans-acting polypeptide responsible for stimulation of immediate early transcription. *J. Mol. Biol.* **180**, 1-19.
9. Sadowski, I., Ma, J., Triezenberg, S. and Ptashne, M. (1988) GAL4-VP16 is an unusually potent transcriptional activator. *Nature* **335**, 563-564.
10. Regier, J. L., Shen, F. and Triezenberg, S. J. (1993) Pattern of aromatic and hydrophobic amino acids critical for one of two subdomains of the VP16 transcriptional activator. *Proc. Natl. Acad. Sci. U.S.A.* **90**, 883-887.
11. Sullivan, S. M., Horn, P. J., Olson, V. A., Koop, A. H., Niu, W., Ebright, R. H. and Triezenberg, S. J. (1998) Mutational analysis of a transcriptional activation region of the VP16 protein of herpes simplex virus. *Nucleic. Acids. Res.* **26**, 4487-4496.
12. Shen, F., Triezenberg, S. J., Hensley, P., Porter, D. and Knutson, J. R. (1996) Transcriptional activation domain of the herpesvirus protein VP16 becomes conformationally constrained upon interaction with basal transcription factors. *J. Biol. Chem.* **271**, 4827-4837.
13. Kobayashi, N., Boyer, T. G. and Berk, A. J. (1995) A class of activation domains interacts directly with TFIIA and stimulates TFIIA-TFIID-promoter complex assembly. *Mol. Cell. Biol.* **15**, 6465-6473.
14. Kobayashi, N., Horn, P. J., Sullivan, S. M., Triezenberg, S.

J., Boyer, T. G. and Berk, A. J. (1998) DA-complex assembly activity required for VP16C transcriptional activation. *Mol. Cell. Biol.* **18**, 4023-4031.
15. Hardy, S., Brand, M., Mittler, G., Yanagisawa, J., Kato, S., Meisterernst, M. and Tora, L. (2002) TATA-binding protein-free TAF-containing complex (TFTC) and p300 are both required for efficient transcriptional activation. *J. Biol. Chem.* **277**, 32875-32882.
16. Ikeda, K., Stuehler, T. and Meisterernst, M. (2002) The H1 and H2 regions of the activation domain of herpes simplex virion protein 16 stimulate transcription through distinct molecular mechanisms. *Genes Cells* **7**, 49-58.
17. Kraus, W. L., Manning, E. T. and Kadonaga, J. T. (1999) Biochemical analysis of distinct activation functions in p300 that enhance transcription initiation with chromatin templates. *Mol. Cell. Biol.* **19**, 8123-8135.
18. Kundu, T. K., Palhan, V. B., Wang, Z., An, W., Cole, P. A. and Roeder, R. G. (2000) Activator-dependent transcription from chromatin *in vitro* involving targeted histone acetylation by p300. *Mol. Cell* **6**, 551-561.
19. Uesugi, M., Nyanguile, O., Lu, H., Levine, A. J. and Verdine, G. L. (1997) Induced alpha helix in the VP16 activation domain upon binding to a human TAF. *Science* **277**, 1310-1313.
20. Klemm, R. D., Goodrich, J. A., Zhou, S. and Tjian, R. (1995) Molecular cloning and expression of the 32-kDa subunit of human TFIID reveals interactions with VP16 and TFIIB that mediate transcriptional activation. *Proc. Natl. Acad. Sci. U.S.A.* **92**, 5788-5792.
21. Burley, S. K. and Roeder, R. G. (1996) Biochemistry and structural biology of transcription factor IID (TFIID). *Annu. Rev. Biochem.* **65**, 769-799.
22. Choi, Y., Asada, S. and Uesugi, M. (2000) Divergent hTAFII31-binding motifs hidden in activation domains. *J. Biol. Chem.* **275**, 15912-15916.
23. Langlois, C., Mas, C., Di Lello, P., Jenkins, L. M., Legault, P. and Omichinski, J. G. (2008) NMR structure of the complex between the Tfb1 subunit of TFIIH and the activation domain of VP16: structural similarities between VP16 and p53. *J. Am. Chem. Soc.* **130**, 10596-10604.
24. Jonker, H. R., Wechselberger, R. W., Boelens, R., Folkers, G. E. and Kaptein, R. (2005) Structural properties of the promiscuous VP16 activation domain. *Biochemistry* **44**, 827-839.
25. Chi, S. W., Lee, S. H., Kim, D. H., Ahn, M. J., Kim, J. S., Woo, J. Y., Torizawa, T., Kainosho, M. and Han, K. H. (2005) Structural details on mdm2-p53 interaction. *J. Biol. Chem.* **280**, 38795-38802.
26. Bochkareva, E., Kaustov, L., Ayed, A., Yi, G. S., Lu, Y., Pineda-Lucena, A., Liao, J. C., Okorokov, A. L., Milner, J., Arrowsmith, C. H. and Bochkarev, A. (2005) Single-stranded DNA mimicry in the p53 transactivation domain interaction with replication protein A. *Proc. Natl. Acad. Sci. U.S.A.* **102**, 15412-15417.
27. Di Lello, P., Jenkins, L. M., Jones, T. N., Nguyen, B. D., Hara, T., Yamaguchi, H., Dikeakos, J. D., Appella, E., Legault, P. and Omichinski, J. G. (2006) Structure of the Tfb1/p53 complex: Insights into the interaction between the p62/Tfb1 subunit of TFIIH and the activation domain of p53. *Mol. Cell* **22**, 731-740.
28. Lee, S. H., Park, K. H., Kim, D. H., Choung, D. H., Suk, J. E., Kim, D. H., Chang, J., Sung, Y. C., Choi, K. Y. and Han, K. H. (2001) Structural origin for the transcriptional activity of human p53. *J. Biochem. Mol. Biol.* **34**, 73-79.
29. O'Hare, P. and Williams, G. (1992) Structural studies of the acidic transactivation domain of the Vmw65 protein of herpes simplex virus using 1H NMR. *Biochemistry* **31**, 4150-4156.
30. Chi, S. W., Kim, D. H., Lee, S. H., Chang, I. and Han, K. H. (2007) Pre-structured motifs in the natively unstructured preS1 surface antigen of hepatitis B virus. *Protein Sci.* **16**, 2108-2117.
31. Maeng, C. Y., Oh, M. S., Park, I. H. and Hong, H. J. (2001) Purification and structural analysis of the hepatitis B virus preS1 expressed from *Escherichia coli*. *Biochem. Biophys. Res. Commun.* **282**, 787-792.
32. Kim, D. H., Ni, Y., Lee, S. H., Urban, S. and Han, K. H. (2008) An anti-vial peptide derived from the preS1 surface protein of hepatitis B virus. *BMB Rep.* **41**, 640-644.
33. Kussie, P. H., Gorina, S., Marechal, V., Elenbaas, B., Moreau, J., Levine, A. J. and Pavletich, N. P. (1996) Structure of the MDM2 oncoprotein bound to the p53 tumor suppressor transactivation domain. *Science* **274**, 948-953.
34. Demarest, S. J., Martinez-Yamout, M., Chung, J. Chen, H., Xu, W., Dyson, H. J., Evans, R. M. and Wright, P. E. (2002) Mutual synergistic folding in recruitment of CBP/p300 by p160 nuclear receptor coactivators. *Nature* **415**, 549-553.
35. Sayers, E. W., Gerstner, R. B., Draper, D. E. and Torchia, D. A. (2000) Structural preordering in the N-terminal region of ribosomal protein S4 revealed by heteronuclear NMR spectroscopy. *Biochemistry* **39**, 13602-13613.
36. Ramelot, T. A., Gentile, L. N. and Nicholson, L. K. (2000) Transient structure of the amyloid precursor protein cytoplasmic tail indicates preordering of structure for binding to cytosolic factors. *Biochemistry* **39**, 2714-2725.
37. Zitzewitz, J. A., Ibarra-Molero, B., Fishel, D. R., Terry, K. L. and Matthews, C. R. (2000) Preformed secondary structure drives the association reaction of GCN4-p1, a model coiled-coil system. *J. Mol. Biol.* **296**, 1105-1116.
38. Bienkiewicz, E. A., Adkins, J. N. and Lumb, K. J. (2002) Functional consequences of preorganized helical structure in the intrinsically disordered cell-cycle inhibitor p27 (Kip1). *Biochemistry* **41**, 752-759.
39. Parker, D., Rivera, M., Zor, T., Henrion-Caude, A., Radhakrishnan, I., Kumar, A., Shapiro, L. H., Wright, P. E., Montminy, M. and Brindle, P. K. (1999) Role of secondary structure in discrimination between constitutive and inducible activators. *Mol. Cell. Biol.* **19**, 5601-5607.
40. Daughdrill, G. W., Hanely, L. J. and Dahlquist, F. W. (1998) The C-terminal half of the anti-sigma factor FlgM contains a dynamic equilibrium solution structure favoring helical conformations. B*iochemistry* **37**, 1076-1082.
41. Domanski, M., Hertzog, M., Coutant, J., Gutsche-Perelroizen, I., Bontems, F., Carlier, M. F., Guittet, E. and van Heijenoort, C. (2004) Coupling of folding and binding of thymosin beta4 upon interaction with monomeric actin monitored by nuclear magnetic resonance. *J. Biol. Chem.* **279**, 23637-23645.
42. Radhakrishnan, I., Perez-Alvarado, G. C., Parker, D., Dyson, H. J., Montminy, M. R. and Wright, P. E. (1997) Solution structure of the KIX domain of CBP bound to the

transactivation domain of CREB: a model for activator:co-activator interactions. *Cell* **91**, 741-752.
43. Chang, J. F., Phillips, K., Lundback, T., Gstaiger, M., Ladbury, J. E. and Luisi, B. (1999) Oct-1 POU and octamer DNA co-operate to recognise the Bob-1 transcription co-activator via induced folding. *J. Mol. Biol.* **288**, 941-952.
44. Kim, A. S., Kakalis, L. T., Abdul-Manan, N., Liu, G. A. and Rosen, M. K. (2000) Autoinhibition and activation mechanisms of the Wiskott-Aldrich syndrome protein. *Nature* **404**, 151-158.
45. Dames, S. A., Martinez-Yamout, M., De Guzman, R. N., Dyson, H. J. and Wright, P. E. (2002) Structural basis for Hif-1 alpha /CBP recognition in the cellular hypoxic response. *Proc. Natl. Acad. Sci. U.S.A.* **99**, 5271-5276.
46. Dyson, H. J. and Wright, P. E. (2002) Coupling of folding and binding for unstructured proteins. *Curr. Opin. Struct. Biol.* **12**, 54-60.
47. Mucsi, Z., Hudecz, F., Hollosi, M., Tompa, P. and Friedrich, P. (2003) Binding-induced folding transitions in calpastatin subdomains A and C. *Protein Sci.* **12**, 2327-2336.
48. De Guzman, R. N., Martinez-Yamout, M. A., Dyson, H. J. and Wright, P. E. (2004) Interaction of the TAZ1 domain of the CREB-binding protein with the activation domain of CITED2: regulation by competition between intrinsically unstructured ligands for non-identical binding sites. *J. Biol. Chem.* **279**, 3042-3049.
49. Dyson, H. J. and Wright, P. E. (2005) Intrinsically unstructured proteins and their functions. *Nat. Rev. Mol. Cell. Biol.* **6**, 197-208.
50. Sugase, K., Dyson, H. J. and Wright. P. E. (2007) Mechanism of coupled folding and binding of an intrinsically disordered protein. *Nature* **447**, 1021-1025.
51. Radhakrishnan, I., Perez-Alvarado, G. C., Dyson, H. J. and Wright, P. E. (1998) Conformational preferences in the Ser133-phosphorylated and non-phosphorylated forms of the kinase inducible transactivation domain of CREB. *FEBS Lett.* **430**, 317-322.
52. Wishart, D. S. and Sykes, B. D. (1994) Chemical shifts as a tool for structure determination. *Methods Enzymol.* **239**, 363-392.